Elastic field in an infinite medium of one-dimensional hexagonal quasicrystal with a planar crack

CrossMark

X.-Y. Li *

School of Mechanics and Engineering, Southwest Jiaotong University, Chengdu 610031, PR China

A R T I C L E   I N F O

A B S T R A C T

This present work is concerned with planar cracks embedded in an infinite space of one-dimensional hexagonal quasicrystals. The potential theory method together with the general solutions is used to develop the framework of solving the crack problems in question. The mode I problems of three common planar cracks (a penny-shaped crack, an external circular crack and a half-infinite crack) are solved in a systematic manner. The phonon and phason elastic fundamental fields along with some important parameters in crack analysis are explicitly presented in terms of elementary functions. Several examples are given to show the applications of the present fundamental solutions. The validity of the present solutions is discussed both analytically and numerically. The derived analytical solutions of crack will not only play an important role in understanding the phonon–phason coupling behavior in quasicrystals, but also serve as benchmarks for future numerical studies and simplified analyses.

© 2013 Elsevier Ltd. All rights reserved.

1. Introduction

Quasicrystals (QCs), which are aperiodic but ordered structural forms between crystals and glass, were initially discovered by Shechtman et al. (1984). Since then, the theoretical and experimental studies of QCs have been one of the foci of research in the physics of condensed matter. Up to now, more than 100 different alloys of QCs with stable thermodynamic properties have been produced (Fan and Mai, 2004) and the engineering application of QCs has been found recently, as reinforced phases of polymer-matrix composites (Kenzari et al., 2012).

According to the theory of elasticity based on Landau's theory (Landau and Lifshitz, 1958), the elastic behavior of QCs is described by the phonon and phason fields which are in general anisotropic and coupled to each other (Wang et al., 1997). This definitely brings out a great deal of challenges in mechanical analyses of QCs, and simplifications are therefore made in the previous investigations, especially those for cracks and dislocations (Fan, 2011). In the past three decades, various plane stress and strain problems were investigated, and many methods in classic planar elasticity have been generalized to QCs, for example, Fourier transform (Bochner and Chandrasekharan, 1949), perturbation method (Hinch, 1991), Stroh formulism (Stroh, 1958, 1962) and the complex variable function method developed by Muskhelishvili (1963). By these methods, some problems of crack (Fan et al., 2012), dislocation (Li and Liu, 2012), inclusion (Wang, 2004) and

bimaterials with imperfect interfaces (Gao and Ricoeur, 2010) have been successfully solved. It should be noted that aforementioned solutions are essentially independent of one spatial coordinate. This may not reflect the characteristics of a real problem in practice.

As a result, it is imperative to seek 3D elastic solutions to clarify the simplified analyses. Some scholars have made several developments relative to general solutions (Chen et al., 2004), Green's functions for an infinite space consisting of two materials (Gao and Ricoeur, 2011), axisymmetric crack and indentation problems (Peng and Fan, 2001), the interaction of the phonon and phason fields at a crack tip (Mariano et al., 2004), and non-axisymmetric mode I crack problem in the context of thermo-elasticity of QC (Li, 2013).

According to the review article (Fan and Mai, 2004) and the monograph (Fan, 2011), which comprehensively give the state of the art of investigations on the mechanical analyses of QCs, 3D analytical studies on the crack problems are quite scarce. The research works (Fan, 2011) conducted by Fan and his co-authors by means of Fourier and Hankel transforms are limited to axisymmetric problems and the physical quantities on the crack plane. To the best of authors' knowledge, there is no non-axisymmetric solutions available in the literature, within the framework of elasticity of QC.

From an overall point of view, most of foregoing research work were performed within the linear elasticity of QCs, and did not take self-actions in phason field into account. In some particular cases, the absence of phason self-actions would lead to non-physical results, which was first pointed out by Mariano (2006) and then numerically verified by Colli and Mariano (2011). Furthermore, self-interaction in phason field can be described in the context of nonlinear elasticity of QCs (Mariano, 2006). Recently, Mariano

* Tel.: +86 28 8763 4181; fax: +86 28 8760 0797.
 E-mail address: zjuparis6@hotmail.com

and Planas (2013), on the basis of first invariance principles and within the framework of (both finite and small strain) continuum mechanics of QCs, discussed the existence of a phason self-interaction with both conservative and dissipative components. In this study, however, the assumptions in standard linear elasticity of QC are still accepted, and all the quantities obtained make a physical sense, as shown later.

The present work is on a penny-shaped crack, an external circular crack and a half-infinite plane crack, each of which is embedded in an infinite space of one-dimensional hexagonal quasi-crystals. The problems of these three typical cracks are classic ones in fracture mechanics and have been extensively investigated in the framework of pure elasticity (Fabrikant, 1989, 1991; Fabrikant and Karapetian, 1994; Fabrikant et al., 1994). In this study, two pairs of equal but opposite phonon and phason loads are applied on the upper and lower crack lips for each crack, and the original problem is transformed into a mixed boundary problem of a half-infinite space. Potential theory method (Fabrikant, 1989, 1991) in cooperation with the general solution (Chen et al., 2004) is employed to solve the resulting mixed boundary problem.

The next sections are organized as follows. In Section 2, we recall the general solutions in terms of quasi-harmonic functions for 3D static problems, which were proposed by Chen et al. (2004) using the rigorous operator theory and generalized Almansi's theorem. In Section 3 dedicated to extention of the potential theory method to the crack analysis of 1D hexagonal QCs, a new potential is introduced to account for the effect of phason field. The constants involved are determined and the boundary integro-differential equations (BIEs) are established using the boundary conditions as well as the properties of simple layer potentials (SLP). Section 4 is concerned with the solution of the BIEs and the exact and complete fundamental solutions expressed in terms of elementary functions. Some important quantities in crack analyses such as stress intensity factor (SIF) and crack surface displacement (CSD) are derived in Section 5. As applications of the present fundamental solutions, three concrete examples are given in Section 6. In Section 7, numerical calculations are performed to show the variations of physical quantities of special interests. Finally, some concluding remarks are drawn in Section 8.

2. General solution of static problem

Consider a 1D hexagonal QC with point groups $6mm, 62_h2_h, \bar{6}_m2_h$ and $6m_hmm$, whose atoms are arranged periodically in the $x - y$ plane and quasi-periodically in the z-direction in a Cartesian coordinate system $Oxyz$. Without the effect of body forces, the equilibrium equations, in terms of the phonon displacements (u_x, u_y, u_z) and the phason degree of freedom (w_z), read (Chen et al., 2004; Fan, 2011)

$$\left(c_{11}\frac{\partial^2}{\partial x^2} + c_{66}\frac{\partial^2}{\partial y^2} + c_{44}\frac{\partial^2}{\partial z^2} \right)u_x + (c_{12} + c_{66})\frac{\partial^2 u_y}{\partial x \partial y}$$
$$+ (c_{13} + c_{44})\frac{\partial^2 u_z}{\partial x \partial z} + (R_1 + R_3)\frac{\partial^2 w_z}{\partial x \partial z} = 0, \tag{1a}$$

$$(c_{12} + c_{66})\frac{\partial^2 u_x}{\partial x \partial y} + \left(c_{66}\frac{\partial^2}{\partial x^2} + c_{11}\frac{\partial^2}{\partial y^2} + c_{44}\frac{\partial^2}{\partial z^2} \right)u_y$$
$$+ (c_{13} + c_{44})\frac{\partial^2 u_z}{\partial y \partial z} + (R_1 + R_3)\frac{\partial^2 w_z}{\partial y \partial z} = 0, \tag{1b}$$

$$(c_{13} + c_{44})\frac{\partial}{\partial z}\left(\frac{\partial u_x}{\partial x} + \frac{\partial u_x}{\partial x} \right) + \left(c_{44}\Delta + c_{33}\frac{\partial^2}{\partial z^2} \right)u_z$$
$$+ \left(R_3\Delta + R_2\frac{\partial^2}{\partial z^2} \right)w_z = 0, \tag{1c}$$

$$(R_1 + R_3)\frac{\partial}{\partial z}\left(\frac{\partial u_x}{\partial x} + \frac{\partial u_y}{\partial x} \right) + \left(R_3\Delta + R_2\frac{\partial^2}{\partial z^2} \right)u_z$$
$$+ \left(K_2\Delta + K_1\frac{\partial^2}{\partial z^2} \right)w_z = 0 \tag{1d}$$

where $\Delta = \partial^2/\partial x^2 + \partial^2/\partial y^2$ is the plane Laplacian; c_{ij}, K_i and R_i are, respectively, phonon, phason and phonon–phason coupling elastic constants.

Physically, phason degree of freedom appears as a result of the quasi-periodic symmetric of QCs. Phason degrees of freedom describe the atomic jump from one location to another one nearby bearing a similar local environment or rearrangement of atoms from one potential valley to another, which will break the quasi-periodic symmetric property of QCs and change the system elastic energy (Wu et al., 2013). Corresponding to the phason degrees of freedom, there exist phason gradient, stress and force in theory of elasticity of QC (Fan, 2011).

It should be pointed out that the conservative component of the inner self-action as shown in Mariano (2006) in the phason field is not considered in (1d), which may result in non-physical results as evidenced by Colli and Mariano (2011). However, the topic is beyond the scope of the present study, and the common assumptions are accepted as in the recent advances for static problems (Fan et al., 2012; Gao and Ricoeur, 2011; Li, 2013) and dynamic problems (Fan et al., 2012; Radi and Mariano, 2011).

The general solutions to the partial differential equations in (1) depend on the eigenvalues $s_i(i = 1, 2, 3)$, which are roots, with positive real parts $[Re(s_i) > 0]$, of the following characteristic equation (Chen et al., 2004)

$$as^6 - bs^4 + cs^2 - d = 0, \tag{2}$$

where the constants a, b, c and d, related to the material constants c_{ij}, R_i and K_i, are specified by Chen et al. (2004) and are listed in Appendix A. From a physical point of view, the eigen-values s_i characterize the anisotropy degree of the material under consideration.

Chen et al. (2004), using the operator theory and generalized Almansi's theorem, gave 3D general solutions in terms of four quasi-harmonic functions ψ_j ($j = 0, 1, 2, 3$), for transversely isotropic materials whose eigenvalues s_j are all distinct. In this case ($s_i \neq s_j$ once $i \neq j$), the general solutions take in the simplest forms:

$$U = -\bigwedge\left(\sum_{j=1}^{3}\psi_j + i\psi_0 \right), \quad u_{zm} = \sum_{j=1}^{3}\alpha_{mj}\frac{\partial \psi_j}{\partial z_j}, \quad (m = 1, 2), \tag{3}$$

with $z_j = zs_j$ $(j = 1, 2, 3), i = \sqrt{-1}$ (without specification elsewhere), $\bigwedge = \partial/\partial x + i\partial/\partial y, U \equiv u_x + iu_y, u_{z1} \equiv u_z$ and $u_{z2} \equiv w_z$. In addition, the constants α_{mj} are defined by Chen et al. (2004) and are listed in Appendix A. The potential functions ψ_j ($j = 0, 1, 2, 3$) are required to satisfy

$$\left(\Delta + \frac{\partial^2}{\partial z_j^2} \right)\psi_j = 0 \ (j = 0, 1, 2, 3), \tag{4}$$

with $s_0 = \sqrt{c_{44}/c_{66}}$ and $z_0 = zs_0$.

We can express the stress components in the following compact form

$$\sigma_1 = 2\sum_{j=1}^{3}\varpi_j\frac{\partial^2 \psi_j}{\partial z_j^2}, \quad \sigma_2 = -2c_{66}\bigwedge^2\left(\sum_{j=1}^{3}\psi_j + i\psi_0 \right),$$
$$\sigma_{zm} = \sum_{j=1}^{3}\gamma_{mj}\frac{\partial^2 \psi_j}{\partial z_j^2}, \quad \tau_{zm} = \bigwedge\left(\sum_{j=1}^{3}s_j\gamma_{mj}\frac{\partial \psi_j}{\partial z_j} - is_0\vartheta_m\frac{\partial \psi_0}{\partial z_0} \right), \tag{5}$$

where the constants γ_{mj} and ϖ_j are also given in Appendix A, and the following notations are introduced for the phonon stresses σ_{ij} and the phason stresses H_{ij}

$$\sigma_1 = \sigma_{xx} + \sigma_{yy}, \quad \sigma_2 = \sigma_{xx} - \sigma_{yy} + 2i\sigma_{xy}, \quad \sigma_{z1} = \sigma_{zz},$$
$$\sigma_{z2} = H_{zz}, \quad \tau_{z1} = \sigma_{zx} + i\sigma_{zy}, \quad \tau_{z2} = H_{zx} + iH_{zy}. \tag{6}$$

In addition, the index m ranges from 1 to 2 hereafter.

The general solutions in (3) and (5) have been proven to be completed as done by Gao et al. (2009). Based on the general solutions and the potential theory method presented by Fabrikant (1989, 1991), we can tackle many non-classic crack problems, as pointed out by Li (2013) in the recent study for 1D QCs under thermal loadings.

3. Generalized potential theory method for crack problem

Consider an infinite space of 1D hexagonal QCs weakened by a planar crack in parallel to the isotropic plane of the material, which lies in the plane $z = 0$. The crack is subjected to a pair of phonon loads $p_1(x, y)$ and $-p_1(x, y)$, and a pair of phason loads $p_2(x, y)$ and $-p_2(x, y)$, on the upper and lower crack lips (see Fig. 1(a)). For notational convenience, the region occupied by the crack is symbolized by S and the complement of S is denoted by $\overline{S}$, so that $S \cap \overline{S} = \emptyset$ and $S \cup \overline{S} = I$ with I denoting the plane $z = 0$. By symmetry, we need to consider only the boundary value problem (BVP) of the half-space $z \geq 0$ with the following boundary conditions (BCs) on the plane I (Fan, 2011; Peng and Fan, 2001):

$$\sigma_{z1} = p_1(x, y), \quad \sigma_{z2} = p_2(x, y), \quad \forall (x, y) \in S;$$
$$u_{z1} = 0, \quad u_{z2} = 0, \quad \forall (x, y) \in \overline{S};$$
$$\tau_{z1} = 0, \quad \forall (x, y) \in I. \tag{7}$$

The BCs at infinite

$$\sigma_{ij} \to 0, \quad H_{ij} \to 0, \quad \forall \sqrt{x^2 + y^2 + z^2} \to \infty \tag{8}$$

must be met as well.

Although no experiments have been reported yet on how to impose the phason loads, within the theory of elasticity of QC (Fan, 2011), however, traction in the phason field must exist on the boundary of a QC, from a theoretical point of view. Hence, we, from the perspective of theoretical study, set on the crack lips $\sigma_{z2} = p_2(x, y)$, in this paper, in which $p_2(x, y)$ can either vanish or be a function of x and y. Such a setting is without losing any generality. In fact, Gao and Ricoeur (2011) used a similar boundary conditions regarding phason force, during the course of derivation of Green's functions for two-dimensional quasi-crystal bimaterials. Of course, the boundary condition relative to phason field should be verified by future experiments.

The sole external boundary condition on phason traction, that appears to be reasonable in terms of phason stress is $\sigma_{z2} = 0$. From the perspective of continuum modeling, in fact, the degrees of freedom included in the phason field "internal" to material elements identified with points in space. The same phason actions appear often as about 1% perturbations of the standard stress field. Therefore, it is hard (even impossible, probably) to control them directly from the exterior, at the macroscopic scale.

To solve the above BVP, we assume that

$$\psi_0 = 0, \quad \psi_j = d_{j1}\Psi_1(z_j) + d_{j2}\Psi_2(z_j) \ (j = 1, 2, 3), \tag{9}$$

where d_{ij} are constants to be determined and $\Psi_m(z)$ are defined by

$$\Psi_m(z) = \Psi_m(M) = \int \int_S \frac{\Omega_m(N_0) dS_0}{R(M, N_0)}, \tag{10}$$

with $dS_0 = dx_0 dy_0$, $R(M, N_0)$ denoting the distance between $M(x, y, z)$ and $N_0(x_0, y_0, 0)$, and $\Omega_m = u_{zm}(x, y, 0)$ being the crack surface displacements (CSDs) in the phonon and phason field, respectively. Furthermore, $\Psi_m(z)$ are simple layer potentials (SLPs) with the property (Fabrikant, 1989, 1991; Kellogg, 1929)

$$\frac{\partial \Psi_m(z)}{\partial z}\Big|_{z=0} = \begin{cases} -2\pi\Omega_m, & (x, y) \in S \\ 0, & (x, y) \in \overline{S} \end{cases}. \tag{11}$$

Observe that (4) and (8) are verified by the potentials in (9), in view of the property of the harmonic function $1/R(M, N_0)$ (Kellogg, 1929). As a consequence, our concern in what follows is about the satisfaction of the BCs prescribed by (7).

The satisfaction of (8) is of physical significance. As pointed out in Section 2, the exclusion of a conservative self-action may lead to meaningless results, from a physical point of view (Colli and Mariano, 2011). This crucial remark was first reported by Mariano (2006) and then evidenced by Colli and Mariano (2011). Owing to the absence of the self-action conservative components, the the dimensionless displacement in phason field at infinity would be divergent (Colli and Mariano, 2011). Now, (8) is checked to avoid failing into such a non-physical situation.

It can be readily verified that all the homogeneous BCs in (7) have been met upon letting

$$\begin{bmatrix} d_{1m} \\ d_{2m} \\ d_{3m} \end{bmatrix} = -\frac{1}{2\pi} \begin{bmatrix} s_1\gamma_{11} & s_2\gamma_{12} & s_3\gamma_{13} \\ \alpha_{11} & \alpha_{12} & \alpha_{13} \\ \alpha_{21} & \alpha_{22} & \alpha_{23} \end{bmatrix}^{-1} \begin{bmatrix} 0 \\ \delta_{1m} \\ \delta_{2m} \end{bmatrix}, \tag{12}$$

with δ_{im} being the Kronecker delta

Accounting for the first condition in (7), we can derive the following two boundary integro-differential equations (BIEs)

$$-\left(\sum_{i=1}^{2} g_{mi} \right) \Delta \int \int_S \frac{\Omega_i(N_0)}{R(N, N_0)} dS_0 = p_m(N), \tag{13}$$

where

$$g_{mi} = \sum_{k=1}^{3} \gamma_{mk} d_{ki}, \tag{14}$$

and $R(N, N_0)$ is the distance between the points $N(x, y, 0) \in S$ and $N_0(x_0, y_0, 0) \in S$. Next, we can rewrite (13) as

$$\Delta \int \int_S \frac{\Omega_m(N_0)}{R(N, N_0)} dS_0 = F_m(N), \tag{15}$$

where $F_j(N)$ are generalized loadings

$$F_1(N) \equiv \frac{g_{12}p_2(N) - g_{22}p_1(N)}{A}, \quad F_2(N) \equiv \frac{g_{21}p_1(N) - g_{11}p_2(N)}{A}, \tag{16}$$

with $A = g_{11}g_{22} - g_{12}g_{21}$.

For an irregular plane crack, we have established two BIEs in (15) bearing the same mathematical structure, which can be in general solved only numerically. However, for some special crack configurations, (15) is expected to have analytical solutions by using the results of potential theory method. Hereafter, our attention will be paid to the aforementioned three common cracks, in the following sections, where the cylindrical coordinate system (r, θ, z) and the Cartesian coordinate system (x, y, z), for convenience, are employed for circular and half-infinite plane cracks, respectively.

4. Fundamental elastic field

Assume that the planar cracks are located on the plane $z = 0$, and the regions occupied by the cracks are symbolized by $S \equiv \{(r, \theta) | r \leq a, 0 \leq \theta \leq 2\pi\}$ for the penny-shaped crack of radius a, by $S \equiv \{(r, \theta) | r \geq a, 0 \leq \theta \leq 2\pi\}$ for the external circular crack with an interior radius a, and by $S \equiv \{(x, y) | -\infty < x < +\infty, y \geq 0\}$ for the half-infinite crack (see Fig. 1(b)–(d)). For the three common planar cracks, the solutions to the BIEs in (15) can be analytically obtained by virtue of the potential theory method,
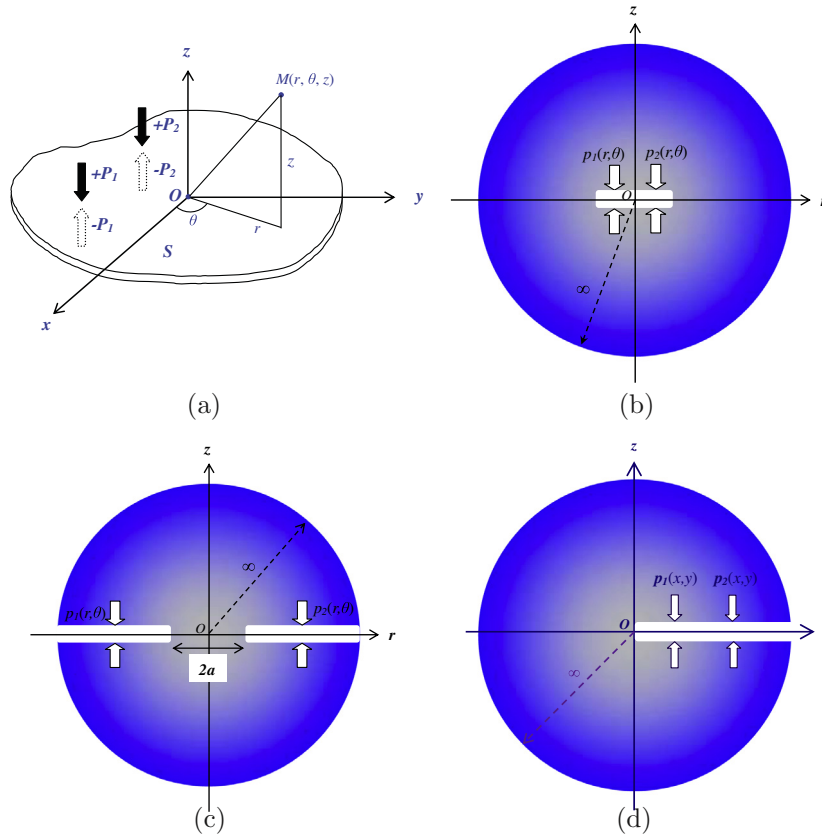
Fig. 1. Schematic figures of a planar crack (a) and of the vertical cross sections of the three common cracks: penny-shaped crack (b), external circular crack (b) and half-infinite crack (d). Two pairs of opposite concentrated forces $\pm P_1$ (phonon) and $\pm P_2$ (phason) acting on the lips of a flat crack S perpendicular to the z axis common to the polar coordinate system (r, θ, z) and the Cartesian coordinate system (x, y, z).

namely, Fabrikant (1989, 1991) for penny-shaped crack, Fabrikant et al. (1994) for external crack and Fabrikant and Karapetian (1994) for the half-infinite crack. Substituting the resultant expressions for Ω_m into (10), we determine the SLPs $\Psi_m(z)$ as

$$\Psi_m(z) = -\frac{1}{2\pi^3} \int \int_S K(M; N_0) F_m(N_0) r_0 dr_0 d\theta_0, \tag{17}$$

where $K(M; N_0)$ is the Green's function (Fabrikant, 1989, 1991; Fabrikant and Karapetian, 1994; Fabrikant et al., 1994)

$$K(M; N_0) = \int \int_S \frac{1}{R(N_\rho, N_0)} \arctan\left[\frac{\eta(N_\rho, N_0)}{R(N_\rho, N_0)}\right] \frac{dS_\rho}{R(M, N_\rho)}, \tag{18}$$

with $dS_\rho = \rho d\rho d\phi = dx_0 dy_0$, and

$$\eta(N, N_\rho) = \begin{cases} \sqrt{a^2 - r^2}\sqrt{a^2 - \rho^2}/a & \text{penny-shaped,} \\ \sqrt{r^2 - a^2}\sqrt{\rho^2 - a^2}/a & \text{external circular,} \\ 2\sqrt{yy_0} & \text{half-infinite plane,} \end{cases} \tag{19}$$

with N_ρ denoting the point $(\rho, \phi, 0)$ for the circular cracks and $(x_0, y_0, 0)$ for the half-infinite crack. Although the integral in (18) is difficult to explicitly figure out, the various derivatives of $K(M; N_0)$, necessary to construct the 3D fundamental elastic fields, can be found in Fabrikant (1989) and are listed in Appendix B.

As shown in Fig. 1, consider that two pairs of equal but opposite concentrated phonon forces $\pm P_1$ and phason forces $\pm P_2$ are respectively applied at the points $N_1(r_1, \theta_1, 0^\pm)$ $[N_1(x_1, y_1, 0^\pm)]$ and $N_2(r_2, \theta_2, 0^\pm)$ $[N_2(x_2, y_2, 0^\pm)]$ on the crack lips of circular cracks (half-infinite crack), i.e., $p_m(r, \theta) = P_m \delta(r - r_m)\delta(\theta - \theta_m)/r$, $[p_m(x, y) = P_m \delta(x - x_m)\delta(y - y_m)]$. The exact and fundamental elastic field in the half-space $z \geqslant 0$ induced by the external forces can be

figured out by inserting the Green's function in (18) and its derivatives in Appendix B to (3) and (5). In terms of elementary functions, corresponding fundamental field to the three cracks can be uniformly expressed as

$$U = \frac{1}{\pi^2 A} \sum_{i=1}^{2}\sum_{j=1}^{3} P_{ij}^0 f_{1i}^{(k)}(z_j), \quad u_{zm} = -\frac{1}{\pi^2 A} \sum_{i=1}^{2}\sum_{j=1}^{3} P_{ij}^0 \alpha_{mj} f_{2i}^{(k)}(z_j),$$

$$\sigma_1 = -\frac{2}{\pi^2 A} \sum_{i=1}^{2}\sum_{j=1}^{3} P_{ij}^0 \varpi_j f_{3i}^{(k)}(z_j), \quad \sigma_2 = \frac{2c_{66}}{\pi^2 A} \sum_{i=1}^{2}\sum_{j=1}^{3} P_{ij}^0 f_{4i}^{(k)}(z_j), \tag{20}$$

$$\sigma_{zm} = -\frac{1}{\pi^2 A} \sum_{i=1}^{2}\sum_{j=1}^{3} P_{ij}^0 \gamma_{mj} f_{3i}^{(k)}(z_j), \quad \tau_{zm} = -\frac{1}{\pi^2 A} \sum_{i=1}^{2}\sum_{j=1}^{3} P_{ij}^0 s_j \gamma_{mj} f_{5i}^{(k)}(z_j),$$

with

$$P_{1j}^0 = P_1(d_{j2}g_{21} - d_{j1}g_{22}), \quad P_{2j}^0 = P_2(d_{j1}g_{12} - d_{j2}g_{11}). \tag{21}$$

The superscript $k = p, e$ and h of the functions in (20) indicates the penny-shaped, external circular and half-infinite cracks, respectively. In (20), functions $f_{jm}^{(k)}(z)$ $(j = 1, 2, \ldots, 5)$ is equal to $f_j^{(k)}(r, \theta, z; r_m, \theta_m)$ for circular crack and $f_j^{(k)}(x, y, z; x_m, y_m)$ for the half-infinite crack, and all these functions, directly related to the derivatives of the Green's function in (18), are specified in Appendix B.

In the physical context of the present paper, the fundamental solutions (20) reflect, in particular, the effects of the phonon–phson coupling on the elastic fields in a 1D hexagonal QC body weakened by a flat crack.

5. Stress intensity factor and crack surface displacement

Since the fundamental solutions have been derived explicitly in the last section, it is ready to obtain some important quantities associated with the crack. In what follows, we derive the stress intensity factors (SIFs) and crack surface displacements (CSDs) for the three cracks.

5.1. Penny-shaped crack

In view of the properties specified in (B-3), we can deduce that

$$f_2^{(p)}(N;N_0) = -\frac{1}{R(N,N_0)} \arctan \frac{\eta(N,N_0)}{R(N,N_0)}, \quad N \in S,$$

$$f_3^{(p)}(N;N_0) = -\sqrt{\frac{a^2 - r_0^2}{r^2 - a^2}} \frac{1}{R^2(N,N_0)}, \quad N \in \overline{S}. \tag{22}$$

Thus, the normal stress components at the point $N(r,\theta,0) \in \overline{S}$ are given by

$$\sigma_{zm}(r,\theta,0) = \sum_{i=1}^{2} P_i B_{mi} \sqrt{\frac{a^2 - r_i^2}{r^2 - a^2}} \frac{1}{r^2 + r_i^2 - 2rr_i \cos(\theta - \theta_i)}, \tag{23}$$

where the constants are specified by

$$B_{m1} = \frac{1}{\pi^2 A} \sum_{j=1}^{3} \gamma_{mj}(d_{j2}g_{21} - d_{j1}g_{22}),$$

$$B_{m2} = \frac{1}{\pi^2 A} \sum_{j=1}^{3} \gamma_{mj}(d_{j1}g_{12} - d_{j2}g_{11}). \tag{24}$$

With the aid of (14), we can derive the normal stress components outside the crack as

$$\sigma_{zm}(r,\theta,0) = -\frac{P_m}{\pi^2} \sqrt{\frac{a^2 - r_m^2}{r^2 - a^2}} \frac{1}{r^2 + r_m^2 - 2rr_m \cos(\theta - \theta_m)}. \tag{25}$$

It is seen that the normal phonon and phason stresses depend only upon the external phonon load and no interactions between the phonon and phason fields occur in regard to these normal stresses.

Defining the stress intensity factors for mode I crack problems by

$$k_{mI} = \lim_{r \to a} \sqrt{r - a}\, \sigma_{zm}(r,\theta,0), \tag{26}$$

we get

$$k_{mI} = -\frac{P_m}{\sqrt{2a}\pi^2} \frac{\sqrt{a^2 - r_m^2}}{a^2 + r_m^2 - 2ar_m \cos(\theta - \theta_m)}. \tag{27}$$

It is clearly shown that the SIFs, independent of the material properties, are related to the magnitudes and positions of the external loadings.

The CSDs $\Omega_m = u_{zm}(r,\theta,0)$ can be derived from (20) and (22) as

$$u_{zm}(r,\theta,0) = -\frac{1}{\pi^2 A} \left(\sum_{j=1}^{3} P_{1j}^0 \alpha_{mj} \right) f_{21}^{(p)}(0)$$
$$- \frac{1}{\pi^2 A} \left(\sum_{j=1}^{3} P_{2j}^0 \alpha_{mj} \right) f_{22}^{(p)}(0), \tag{28}$$

where $f_{2m}^{(p)}(0) = f_2^{(p)}(r,\theta,0;r_m,\theta_m)$. Using the relations in (21) and (12), we can simplify (28) as

$$\Omega_1 = -\frac{P_1 g_{22}}{2\pi^3 A} f_{21}^{(p)}(0) + \frac{P_2 g_{12}}{2\pi^3 A} f_{22}^{(p)}(0), \quad \Omega_2$$
$$= \frac{P_1 g_{21}}{2\pi^3 A} f_{21}^{(p)}(0) - \frac{P_2 g_{11}}{2\pi^3 A} f_{22}^{(p)}(0). \tag{29}$$

5.2. External circular crack

To obtain the SIFs and CSDs, we need the behaviors of two functions $f_2^{(e)}(z)$ and $f_3^{(e)}(z)$ when z tends to zero. From (B-4b), (B-4c) and (B-6), it is seen that

$$f_2^{(e)}(N;N_0) = -\frac{1}{R(N,N_0)} \arctan \frac{J(N,N_0)}{R(N,N_0)} N \in S,$$

$$f_3^{(e)}(N;N_0) = -\sqrt{\frac{r_0^2 - a^2}{a^2 - r^2}} \frac{1}{R^2(N,N_0)} N \in \overline{S}, \tag{30}$$

where

$$J(N,N_0) = \sqrt{(r^2 - a^2)(r_0^2 - a^2)}/a. \tag{31}$$

We can obtain the generalized normal stresses in the crack neck $\overline{S}$ as

$$\sigma_{zm}|_{z=0} = \sum_{i=1}^{2} P_i B_{mi} \sqrt{\frac{r_i^2 - a^2}{a^2 - r^2}} \frac{1}{r^2 + r_i^2 - 2rr_i \cos(\theta - \theta_m)}. \tag{32}$$

By means of (14), (32) is simplified as

$$\sigma_{zm}|_{z=0} = -\frac{P_m}{\pi^2} \sqrt{\frac{r_m^2 - a^2}{a^2 - r^2}} \frac{1}{r^2 + r_m^2 - 2rr_m \cos(\theta - \theta_m)}. \tag{33}$$

Introducing the stress intensity factors of mode I

$$k_{mI} = \lim_{r \to a} \sqrt{a - r}\, \sigma_{zm}(r,\theta,0), \tag{34}$$

to describe the singularities at the crack tip, we obtain from (33) that

$$k_{mI} = -\frac{P_m}{\pi^2 \sqrt{2a}} \frac{\sqrt{r_m^2 - a^2}}{a^2 + r_m^2 - 2ar_m \cos(\theta - \theta_m)}. \tag{35}$$

From (20) and (39), the CSDs are determined as

$$\Omega_m = -\frac{1}{\pi^2 A} \left(\sum_{j=1}^{3} P_{1j}^0 \alpha_{mj} \right) f_{21}^{(e)}(0) - \frac{1}{\pi^2 A} \left(\sum_{j=1}^{3} P_{2j}^0 \alpha_{mj} \right) f_{22}^{(e)}(0), \tag{36}$$

with $f_{2m}^{(e)}(0) = f_2^{(e)}(r,\theta,0;r_m,\theta_m)$ Taking advantage of the relations in (21) and (12), we simplify (36) as

$$\Omega_1 = -\frac{P_1 g_{22}}{2\pi^3 A} f_{21}^{(e)}(0) + \frac{P_2 g_{12}}{2\pi^3 A} f_{22}^{(e)}(0),$$

$$\Omega_2 = \frac{P_1 g_{21}}{2\pi^3 A} f_{21}^{(e)}(0) - \frac{P_2 g_{11}}{2\pi^3 A} f_{22}^{(e)}(0). \tag{37}$$

5.3. Half-infinite plane crack

From (B-8), it is easy to get that

$$\lim_{z \to 0} l_1^* = \min(y,0), \quad \lim_{z \to 0} l_2^* \to \max(y,0),$$

$$\lim_{z \to 0} h^* = 2\sqrt{y_0 \max(y,0)}, \quad \lim_{z \to 0} \frac{z}{h^*} = \sqrt{-\frac{\min(y,0)}{y_0}}. \tag{38}$$

By virtue of (B-7b), (B-7c) and (38), we arrive at

$$f_2^{(h)}(0) = -\frac{1}{R(N,N_0)} \arctan \frac{\eta(N,N_0)}{R(N,N_0)}, \quad (y > 0),$$

$$f_3^{(h)}(0) = -\frac{1}{R^2(N,N_0)} \sqrt{\frac{y_0}{-y}}, \quad (y < 0). \tag{39}$$

Thus the generalized normal stresses in the region $\overline{S}$ $(y < 0)$ are obtained as

$$\sigma_{zm}(x,y,0) = \sum_{i=1}^{2} P_i B_{mi} \sqrt{\frac{y_i}{-y}} \frac{1}{(x - x_i)^2 + (y - y_i)^2}. \tag{40}$$

In view of (14), (54) is recast into

$$\sigma_{zm}(x,y,0) = -\frac{P_m}{\pi^2}\sqrt{\frac{y_m}{-y}}\frac{1}{(x-x_m)^2 + (y-y_m)^2}. \tag{41}$$

Defining the SIFs of mode I crack problem

$$k_{mI} = \lim_{y\to 0^-}\sqrt{-y}\,\sigma_{zm}(x,y,0), \tag{42}$$

we immediately get

$$k_{mI} = -\frac{P_m}{\pi^2}\frac{\sqrt{y_m}}{(x-x_m)^2 + y_m^2}. \tag{43}$$

The CSDs $\Omega_m = u_m(x,y,0)$ can be obtained from (39) and (20). Without details, they read

$$\Omega_1 = -\frac{P_1 g_{22}}{2\pi^3 A}f_{21}^{(h)}(0) + \frac{P_2 g_{12}}{2\pi^3 A}f_{22}^{(h)}(0),$$
$$\Omega_2 = \frac{P_1 g_{21}}{2\pi^3 A}f_{21}^{(h)}(0) - \frac{P_2 g_{11}}{2\pi^3 A}f_{22}^{(h)}(0), \tag{44}$$

with $f_{2m}^{(h)}(0) = f_2^{(h)}(x,y,0;x_m,y_m)$.

For arbitrary distributed phonon and phason loads $p_m(x,y)$, the corresponding physical quantities of interest can be obtained by integrating the relative fundamental results over the crack surface. We present three typical examples, which are classic problems and are often solely investigated in literature, in the next section, where distributive loads are considered to be applied on the crack lips.

6. Application of the fundamental solution

6.1. Uniformly loaded penny-shaped crack

Consider case where the crack is under the action of two pairs of equal but opposite pressures $\pm p_1^0$ (phonon) and $\pm p_2^0$ (phason), which are uniformly distributed over the crack lips, namely, $p_1(r,\theta) = p_1^0$, $p_2(r,\theta) = p_2^0$, $\mathsf{F}_1^0 \equiv \mathsf{F}_1(N) = (g_{12}p_2^0 - g_{22}p_1^0)/A$ and $\mathsf{F}_2^0 \equiv \mathsf{F}_2(N) = (g_{21}p_1^0 - g_{11}p_2^0)/A$.

The problem in question is thus axisymmetric. Under this circumstance, the generalized normal stresses Σ_{zm} at the crack front, which are independent of θ, can be derived by integrating the fundamental solutions in (25)

$$\sigma_{zm}(r,\theta,0) = -\frac{p_m^0}{\pi^2}\int_0^a \sqrt{\frac{a^2 - r_m^2}{r^2 - a^2}}r_m dr_m$$
$$\int_0^{2\pi}\frac{d\theta_m}{r^2 + r_m^2 - 2rr_m\cos(\theta - \theta_m)}. \tag{45}$$

Taking advantage of the following identity,

$$\frac{1}{2\pi}\int_0^{2\pi}\frac{x^2 - y^2}{x^2 + y^2 - 2xy\cos(\theta - \theta_0)}d\theta_0 = 1 \ (x > y > 0), \tag{46}$$

we can obtain that

$$\sigma_{zz}|_{z=0} = \frac{2p_1^0}{\pi}\left[\arcsin\frac{a}{r} - \frac{a}{\sqrt{r^2 - a^2}}\right],$$
$$H_{zz}|_{z=0} = \frac{2p_2^0}{\pi}\left[\arcsin\frac{a}{r} - \frac{a}{\sqrt{r^2 - a^2}}\right]. \tag{47}$$

Then, the SIFs can be obtained from (53) and (26) as

$$k_{mI} = -\frac{\sqrt{2a}}{\pi}p_m^0. \tag{48}$$

It is noted that (48) can be retrieved by integrating (27) with the help of (46).

Following a similar procedure, the CSDs for the uniformly loaded crack can be deduced via integration of (63). Without details, they turn out to be

$$\Omega_m(r) = u_{zm}(r,\theta,0) = -\frac{\mathsf{F}_m^0}{\pi^2}\sqrt{a^2 - r^2}, \tag{49}$$

which can be directly recovered by solving the (BIEs) (Fabrikant, 1989)

$$\triangle\int_0^{2\pi}d\theta_0\int_0^a\frac{\Omega_m(r_0,\theta_0)}{\sqrt{r^2 + r_0^2 - 2rr_0\cos(\theta - \theta_0)}}r_0 dr_0 = \mathsf{F}_m^0.$$

Since the problem is axisymmetric and the crack front always keeps the shape of a circle concentric to the original one in the plane $z = 0$, the energy release rate (ERR) is invariant along the crack front. Prior to presenting the ERR, we have to examine the asymptotic behavior of the elastic quantities around the crack tip. Letting $\rho_0 = |r - a| \to 0$, we can obtain the following asymptotic expressions

$$\sigma_{zz}^s(\rho_0) = -\frac{p_1^0}{\pi}\sqrt{\frac{2a}{\rho_0}}, \ \ H_{zz}^s(\rho_0) = -\frac{p_2^0}{\pi}\sqrt{\frac{2a}{\rho_0}},$$
$$\Omega_1^s(\rho_0) = -\frac{g_{12}p_2^0 - g_{22}p_1^0}{\pi^2 A}\sqrt{2a\rho_0}, \Omega_2^s(\rho_0) = -\frac{g_{21}p_1^0 - g_{11}p_2^0}{A}\sqrt{2a\rho_0}. \tag{50}$$

Then, with the help of the concept of crack closure energy (Fan, 2011), the total potential energy release rate is given by

$$\Pi = \lim_{\Delta a\to 0}\frac{1}{\Delta a}\int_0^{\Delta a}\sigma_{zz}^s(\rho_0)\Omega_1^s(\Delta a - \rho_0) + H_{zz}^s(\rho_0)\Omega_2^s(\Delta a - \rho_0)d\rho_0. \tag{51}$$

Substituting (50) into (51) and making use of (48) immediately give rise to

$$\Pi = -\frac{1}{2A}\left[g_{22}k_{1I}^2 + g_{11}k_{2I}^2 - (g_{12} + g_{21})k_{1I}k_{2I}\right]. \tag{52}$$

The first, second and third terms in the brackets attributes to the phonon field, phason field and phonon–phason interactions, respectively.

In principle, the remaining components of the phonon–phason elastic field can be figured out in the same manner described above. However, the integrals involved is very tedious. In Appendix C, we present an alternative way to seek the elastic fields associated with the crack in question.

6.2. External circular crack subjected to annular ring loads

Assume that two pairs of loads $\pm p_1^0$ (phonon) and $\pm p_2^0$ (phason), which are uniformly applied on the annular ring region $a \leqslant b \leqslant r \leqslant c < \infty$. Now the problem is degenerated to an axisymmetric one and all the physical quantities are consequently independent of θ.

The corresponding normal stresses in the crack neck can be obtained by integrating over the annular region

$$\sigma_{zm}|_{z=0} = -\frac{1}{\pi^2}\int_0^{2\pi}d\theta_1\int_b^c\sqrt{\frac{r_1^2 - a^2}{a^2 - r^2}}$$
$$\times\frac{p_m^0 r_1 dr_1}{r^2 + r_1^2 - 2rr_1\cos(\theta - \theta_1)}. \tag{53}$$

Making use of the identity (46), we rewrite (53) as

$$\sigma_{zm}|_{z=0} = \frac{2p_m^0}{\pi}\left[\sqrt{\frac{b^2 - a^2}{a^2 - r^2}} - \arctan\sqrt{\frac{b^2 - a^2}{a^2 - r^2}}\right]$$
$$-\frac{2p_m^0}{\pi}\left[\sqrt{\frac{c^2 - a^2}{a^2 - r^2}} - \arctan\sqrt{\frac{c^2 - a^2}{a^2 - r^2}}\right]. \tag{54}$$

As a consequence, we can derive the SIFs from (34) as

$$k_{mI} = -\frac{p_m^0}{\pi}\sqrt{\frac{2}{a}}\left(\sqrt{c^2 - a^2} - \sqrt{b^2 - a^2}\right), \tag{55}$$

which can be also retrieved by integrating (35).

The CSDs, in this case, can be deduced by integrating the fundamental results in (37) as

$$\Omega_m = -\frac{F_m^0}{\pi^2} I_e(r), \tag{56}$$

where

$$I_e(r) = \frac{1}{2\pi} \int_0^{2\pi} d\theta_0 \int_b^c \frac{1}{R(N, N_0)} \arctan \frac{J(N, N_0)}{R(N, N_0)} r_0 dr_0. \tag{57}$$

The integral (57) can be figured out by following the method proposed by Li (2012) and it turns out to be a continuous function of r

$$I_1(r) = \begin{cases} F_1(r; c, a) - F_1(r; b, a), & a \leqslant r \leqslant b, \\ F_1(r; c, a) - F_2(r; b, a), & b \leqslant r \leqslant c, \\ F_2(r; c, a) - F_2(r; b, a), & c \leqslant r < \infty, \end{cases} \tag{58}$$

where F_1 and F_2 are combinations of elliptic functions defined in Appendix D.

With the previous results, the asymptotic behaviors of the stress and displacement can be derived

$$\sigma_{zz}^s = -\frac{k_{1I}}{\sqrt{\rho_0}}, \quad \Omega_1^s = \frac{(g_{22}k_{1I} - g_{12}k_{2I})}{\pi}\sqrt{\rho_0},$$

$$H_{zz}^s = -\frac{k_{2I}}{\sqrt{\rho_0}}, \quad \Omega_2^s = -\frac{(g_{21}k_{1I} - g_{11}k_{2I})}{\pi}\sqrt{\rho_0}, \tag{59}$$

with $\rho_0 = |a - r| \to 0$. Thus the ERR defined in (51) is of the following form

$$\Pi = -\frac{1}{2A}\left[g_{22}k_{1I}^2 + g_{11}k_{2I}^2 - (g_{12} + g_{21})k_{1I}k_{2I}\right],$$

which is identical to that for penny-shaped crack under the uniform loads.

6.3. Half-infinite crack subjected to linear loads

Let us now consider two pairs of linear loads $\pm P_1^0$ (phonon) and $\pm P_2^0$ (phason) applied along the lines $y = \pm y_m$ ($y_m > 0$), namely, $p_m(x, y) = P_m^0 \delta(y - y_m)$. Thus the crack problem is reduced to an plane strain one and all the physical quantities would be independent of the argument x.

Parallel to the foregoing two cases, we can express $\sigma_{zm}|_{z=0}$ as

$$\sigma_{zm}|_{z=0} = -\frac{1}{\pi^2} \int_{-\infty}^{+\infty} dx_0 \left[\int_0^{+\infty} \sqrt{\frac{y_0}{-y}} \frac{P_m^0 \delta(y_0 - y_m)}{(x - x_0)^2 + (y - y_0)^2} dy_0\right], \tag{60}$$

which can be readily evaluated, with the aid of the property of the Dirac-delta function, as

$$\sigma_{zm}|_{z=0} = -\frac{P_m^0}{\pi(y_m - y)}\sqrt{\frac{y_m}{-y}}, \quad (y < 0, \ y_m > 0). \tag{61}$$

As a consequence, the SIFs are of the form

$$k_{mI} = -\frac{P_m^0}{\pi^2} \int_{-\infty}^{+\infty} \frac{\sqrt{y_m} dx_0}{(x - x_0)^2 + y_m^2} = -\frac{P_m^0}{\pi\sqrt{y_m}}. \tag{62}$$

From (44), we can express the CSDs in the current case as

$$\Omega_1 = -\frac{P_1^0 g_{22}}{2\pi^3 A} \int_{-\infty}^{+\infty} dx_0 \int_0^{+\infty} \delta(y_0 - y_1)f_2^*(0)dy_0$$
$$+ \frac{P_2^0 g_{12}}{2\pi^3 A} \int_{-\infty}^{+\infty} dx_0 \int_0^{+\infty} \delta(y_0 - y_2)f_2^*(0)dy_0,$$

$$\Omega_1 = \frac{P_1^0 g_{21}}{2\pi^3 A} \int_{-\infty}^{+\infty} dx_0 \int_0^{+\infty} \delta(y_0 - y_1)f_2^*(0)dy_0$$
$$- \frac{P_2^0 g_{11}}{2\pi^3 A} \int_{-\infty}^{+\infty} dx_0 \int_0^{+\infty} \delta(y_0 - y_2)f_2^*(0)dy_0. \tag{63}$$

It is evident that the CSDs are dependent of the following integral

$$I_h(y; y_m) = \frac{1}{2\pi}$$
$$\times \int_{-\infty}^{+\infty} dx_0 \left[\int_0^{+\infty} \frac{\delta(y_0 - y_m)}{R(N, N_0)} \arctan \frac{\eta(N, N_0)}{R(N, N_0)} dy_0\right], \tag{64}$$

which seems to be difficult to evaluate. On the other hand, (64) can be transformed into the following form with the help of the results involved in Fabrikant and Karapetian (1994)

$$I_h(y; y_m) = \frac{1}{2} \int_0^y \frac{dt}{\sqrt{y - t}} \int_t^{+\infty} \left[\frac{1}{\sqrt{y_0 - t}} £^*(y + y_0 - 2t)\delta(y_0 - y_m)\right] dy_0, \tag{65}$$

where $£^*(\cdot)$ is an operator defined as

$$£^*(\varrho)f(x, \cdot) = \frac{1}{\pi} \int_{-\infty}^{+\infty} \frac{\varrho f(x_0, \cdot)dx_0}{\varrho^2 + (x - x_0)^2}, \quad \varrho > 0. \tag{66}$$

By virtue of (66), we have

$$£^*(y + y_0 - 2t)\delta(y_0 - y_m) = \delta(y_0 - y_m). \tag{67}$$

Substitution of (67) into (57) yields

$$I_h(y; y_m) = \frac{1}{2} \int_0^y \frac{dt}{\sqrt{y - t}\sqrt{y_m - t}}. \tag{68}$$

Applying the Euler substitution $\sqrt{y - t}\sqrt{y_m - t} = x_0 - t$, we reduce (68) to

$$I_h(y; y_m) = \int_0^{\sqrt{yy_1}} \frac{dx_0}{y + y_m - 2x_0},$$

which is equal to

$$I_h(y; y_m) = \ln \frac{\sqrt{y + y_m}}{|\sqrt{y} - \sqrt{y_m}|}. \tag{69}$$

Consequently, the CSDs turn out to be

$$\Omega_1 = \frac{P_1^0 g_{22}}{\pi^2 A} I(y; y_1) - \frac{P_2^0 g_{12}}{\pi^2 A} I(y; y_2),$$

$$\Omega_2 = -\frac{P_1^0 g_{21}}{\pi^2 A} I(y; y_1) + \frac{P_2^0 g_{11}}{\pi^2 A} I(y; y_2). \tag{70}$$

As expected from a physical point of view, Ω_1 and Ω_2 are logarithmic singular along the lines $y = y_m$, in contrast to the circular cracks exhibiting a square-root singularity.

Similar to the cases of penny-shaped and external circular cracks, we need the asymptotic expressions of stresses and CSDs involved in the definition of ERR (51). From (61) and (70), it is evident that

$$\sigma_{zz}^s = \frac{k_{1I}}{\sqrt{\rho}}, \quad \Omega_1^s = \frac{P_1^0 g_{22}}{\pi^2 A} I_h^s(\rho; y_1) - \frac{P_2^0 g_{12}}{\pi^2 A} I_h^s(\rho; y_2),$$

$$H_{zz}^s = \frac{k_{2I}}{\sqrt{\rho}}, \quad \Omega_2^s = -\frac{P_1^0 g_{21}}{\pi^2 A} I_h^s(\rho; y_1) + \frac{P_2^0 g_{11}}{\pi^2 A} I_h^s(\rho; y_2), \tag{71}$$

with $\rho = |y| \to 0$ and $I_h^s(\rho; y_m) = \ln \frac{\sqrt{y_m}}{\sqrt{y_m} - \sqrt{\rho}}$.

Starting from (51) and making use of the results

$$\lim_{\Delta a \to 0} \frac{1}{\Delta a} \int_0^{\Delta a} \frac{1}{\sqrt{\rho}} \left[\ln \frac{\sqrt{y_m}}{(\sqrt{y_m} - \sqrt{\rho})}\right] d\rho = \frac{\pi}{2\sqrt{y_m}}, \tag{72}$$

we arrive at

$$\Pi = -\frac{1}{2A}\left[g_{22}k_{1I}^2 + g_{11}k_{2I}^2 - (g_{12} + g_{12})k_{1I}k_{2I}\right], \tag{73}$$

which is of the same form as those for penny-shaped and external circular cracks.

7. Numerical results and discussions

This section is devoted to numerically presenting the the foregoing analytical results. To this end, a specific 1D hexagonal QC is considered, with the material properties tubulated in Table 1, by refereing to previous studies (Li, 2013; Radi and Mariano, 2011; Wu et al., 2013). Correspondingly, the eigenvalue s_i ($i = 0, 1, \ldots, 3$), characterizing the anisotropic degree of the materials, have the following the numerical values $s_0 = 1.0260, s_1 = 0.7488 + 0.5177i, s_2 = 0.7488 - 0.5177i$ and $s_3 = 0.5070$, which are different from each other.

For the sake of illustration, the following dimensionless quantities is introduced

$$\xi = \frac{x}{a}, \quad \eta = \frac{y}{a}, \quad \zeta = \frac{z}{a}, \quad r' = \frac{r}{a},$$

$$U'_r = \frac{u_r}{a}, \quad \Omega'_1 = \frac{\Omega_1}{a}, \quad \Omega'_2 = \frac{\Omega_2}{a}, \quad \Sigma_\zeta = \frac{\sigma_{z1}}{c_{11}}, \quad K'_{1I} = \frac{k'_{1I}\sqrt{a}}{c_{11}}.$$

In other words, $a, c_{11}, c_{11}/\sqrt{a}$ are selected as reference scales for spatial coordinates/displacement, stress and stress intensity factors, respectively. Throughout this section, attention is confined to the physical quantities on the crack plane $z = 0$, for simplicity.

7.1. Validity of the present solutions

First, let us first discuss the validity of the present solutions. It is seen from (1) that the phonon–phason coupling effect will vanish by artificially letting R_i be zero. In such a special case, the elastic field resulting from an external mechanical force should be identical to those in the context of pure elasticity. This provides a useful way to check the validity of the present solutions. In this subsection, the validity of the present solutions for circular cracks is discussed by following this path.

Table 2 lists the dimensionless CSD Ω'_1 and the dimensionless normal stress Σ_ζ in the intact region $\bar{S}$, for a penny-shaped crack subjected to a pair of uniform pressures $p_0/c_{11} = 6 \times 10^{-4}$. Comparison of the present solutions is made with in their elastic counterparts, and an excellent agreement is observed.

For the external circular crack, we consider a concentrated phonon force $P_1 = -\pi^2 a^2 c_{11} \times 10^{-6}$ applied at the point $(r'_1, \theta_1) = (2, 0)$ on the crack lip. Similar to the case of the penny-shaped crack, comparison is made with the counterpart given by Fabrikant et al. (1994) in the framework of pure elasticity, as shown in Table 3. Again, the present solutions coincide with those in literature.

It should be pointed out that the data only in Tables 2 and 3 are derived by setting R_i to null. Moreover, the other components of the physical quantities also agree with their counterparts in literature. However, they are omitted for the space-saving purpose.

As far as the half-infinite plane crack is concerned, we adopt another way to check the appropriateness of the solutions. Previous studies (Fabrikant et al., 1993, Fabrikant et al., 1995; Li, 2013) clearly reveal that the fundamental solutions for a half-infinite crack can be extracted from those for the penny-shaped crack, through a limiting procedure.

To fulfill our purpose, we first place the Cartesian coordinate system (x, y, z) at the edge of the circular crack so that

$$x = r\cos\theta, \quad y = r\sin\theta + a, \quad z = z. \tag{75}$$

Then we let the the radius of the circular crack approaches to infinite, i.e., $a \to \infty$. Such a procedure is graphically shown in Fig. 2. In this manner, a half-infinite plane crack is generated and the solutions associated with the circular crack consequently tend to the ones for half-infinite plane crack.

It is noted that the fundamental solutions for penny-shaped and half-infinite cracks are of the same forms. As a result, we need pay our attentions only to the functions $f_j^{(p)}(z)$ and $f_j^{(h)}(z)$ ($j = 1 - 5$) involved in those fundamental solutions. This purpose can be readily achieved by virtue of the following results

$$\lim_{a\to\infty}\frac{a^2 - l_1^2}{a} = 2l_2^*, \quad \lim_{a\to\infty}\frac{l_2^2 - a^2}{a} = -2l_1^*, \quad \lim_{a\to\infty}\frac{a^2 - r_0^2}{a} = 2y_0,$$

$$\lim_{a\to\infty}\frac{s^2}{a} = s^*, \quad \lim_{a\to\infty}h = h^*, \quad \lim_{a\to\infty}\frac{\sqrt{a^2 - r_0^2}}{\bar{s}} = c, \tag{76}$$

where $l_{1,2}, h$ and s are defined in (B-3), and $l_{1,2}^*, h^*, s^*$ and c are given in (B-8). Furthermore, R_0 and t specified by (B-2) keep invariant during the course of limiting procedure.

With the help of (76), we are readily to obtain that

$$\lim_{a\to\infty}f_j^{(p)}(z) = f_j^{(h)}(z), \quad j = 1 - 5 \tag{77}$$

where $f_j^{(h)}(z)$ and $f_j^{(p)}(z)$ are defined in (B-7) and (B-1), respectively.

7.2. Normal stress, SIF and CSD

Consider a penny-shaped crack and an external circular crack, both of which are subjected to a pair of concentrated phonon forces only. The force is assumed to be $P_1 = -\pi^2 a^2 c_{11} \times 10^{-6}$ and is applied at the points $(\xi, \eta, \zeta) = (\lambda, 0, 0^\pm)$. Without specification elsewhere, the parameter $\lambda < 1.0$ for penny-shaped crack is assigned to 0 and 0.5, and $\lambda > 1.0$ for external circular crack is set to 2.0 and 3.0. In this subsection, we only focus on the normal stresses in the region $\bar{S}$ of the crack plane, SIFs and CSDs of the circular cracks.

It is seen from (25) and (33) that the normal stress σ_{zz} in the intact region is independent of the material properties and only a function of r and θ. Its variations are plotted in Fig. 3, which clearly shows that Σ_ζ decrease with r' and θ, for these two circular cracks. As expected, Σ_ζ is singular at the crack front $r' = 1.0$.

To investigate its whole profile, Fig. 4 displays the 3D figure and the contour of Σ_ζ. From an overall point of view, Σ_ζ changes significantly in the neighborhood of the point $(\xi, \eta, \zeta) = (1, 0, 0)$. Furthermore, the symmetry with respect to the x-axis ($y = 0$), associated with the problem in question in this subsection, is checked.

The singularity in Σ_ζ is quantified by the dimensionless stress intensity factor K'_{1I}, whose expression for the circular cracks reads

$$\sqrt{2}K'_{1I} \times 10^6 = \frac{\sqrt{|1 - \lambda^2|}}{1 + \lambda^2 - 2\lambda\cos\theta}.$$

Table 1
Material constants for a particular 1D hexagonal quasi-crystal. (c_{ij}, R_i and K_i in 10^9 Nm^{-2}).

c_{11}	c_{12}	c_{13}	c_{33}	c_{44}
150	55	45	90	50
R_1	R_2	R_3	K_1	K_2
-1.68	1.20	1.20	0.084	0.036

Table 2
The dimensionless displacement and normal stress component for the penny-shaped crack on the crack plane $\zeta = 0$.

$r' = \frac{r}{a}$	$\Omega'_1 \times 10^3$		$r' = \frac{r}{a}$	$\Sigma_\zeta \times 10^3$	
	Present	Fabrikant (1989)		Present	Fabrikant (1989)
0.0	1.179279	1.179279	1.05	0.711432	0.711432
0.2	1.155452	1.155452	1.10	0.397664	0.397664
0.4	1.080827	1.080827	1.15	0.269894	0.269894
0.6	0.943423	0.943423	1.20	0.199560	0.199560
0.8	0.707567	0.707567	1.25	0.155095	0.155095
1.0	0.000000	0.000000	1.30	0.124608	0.124608

Table 3
The dimensionless displacements at the point $(\xi, \eta, \zeta) = (\xi, 0, 0)$ for the external circular crack subjected to a concentrated phonon force exerted at $(r_1', \theta_1) = (2, 0)$.

$\xi = \frac{x}{a}$	$\Omega_1' \times 10^5$		$U_x' \times 10^5$	
	Present	Fabrikant et al. (1994)	Present	Fabrikant et al. (1994)
1.0	0.000000	0.000000	0.230594	0.230594
1.2	0.371466	0.371466	0.249483	0.249483
1.4	0.633399	0.633399	0.301589	0.301589
1.6	1.071278	1.071278	0.421162	0.421162
1.8	2.305933	2.305933	0.797463	0.797463
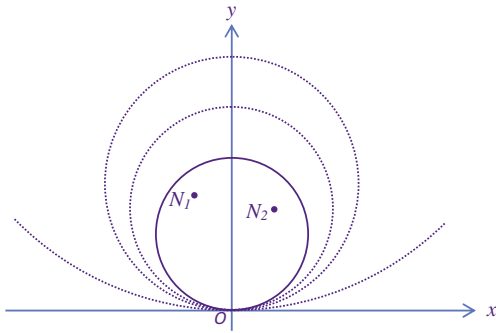
Fig. 2. A schematic figure for the limiting procedure $a \to \infty$. $N_1[x_1(r_1, \theta_1), y_1(r_1, \theta_1)]$ and $N_2[x_2(r_2, \theta_2), y_2(r_2, \theta_2)]$ denote the points at which the concentrated phonon and phason forces are respectively applied on the lips of penny-shaped and half infinite plane cracks.

Since K_{1I}' is independent of the material constants, the SIFs should coincide with their counterparts in the framework of the elasticity.

More specifically, the result for the penny-shaped crack is identical to those predicted by Fabrikant (1989) and the remaining is same to these proposed by Fabrikant et al. (1994). As expected, when the force is applied at the center of the penny-shaped crack, namely, $\lambda = 0$, K_{1I}' is independent of the variable θ because the problem under consideration is axisymmetric. However, in the case of $\lambda > 0$ for circular cracks, the problem is thus non-axisymmetric and K_{1I}' decreases with $\theta \in [0, \pi)$. These characteristics are reflected in Fig. 5.

Fig. 6 illustrates the dimensionless CSD Ω_1' as a function of dimensionless r'. As expected, Ω_1' is singular at the point $(r', \theta, \zeta) = (0.5, 0, 0)$ for the penny-shaped crack and at $(2.0, 0, 0)$ for the external circular crack. Further, Fig. 6 also indicates that Ω_1' decreases with $\theta \in [0, \pi)$.

From (29) and (37), distribution of Ω_2' is similar to that of Ω_1', since they are different from each other only by a constant. Hence, the distribution of the latter is not presented for brevity. Furthermore, under the current circumstance, the ratio between them

$$\alpha = \frac{\Omega_2}{\Omega_1} = -\frac{g_{21}}{g_{11}} = -27.0426 \tag{78}$$

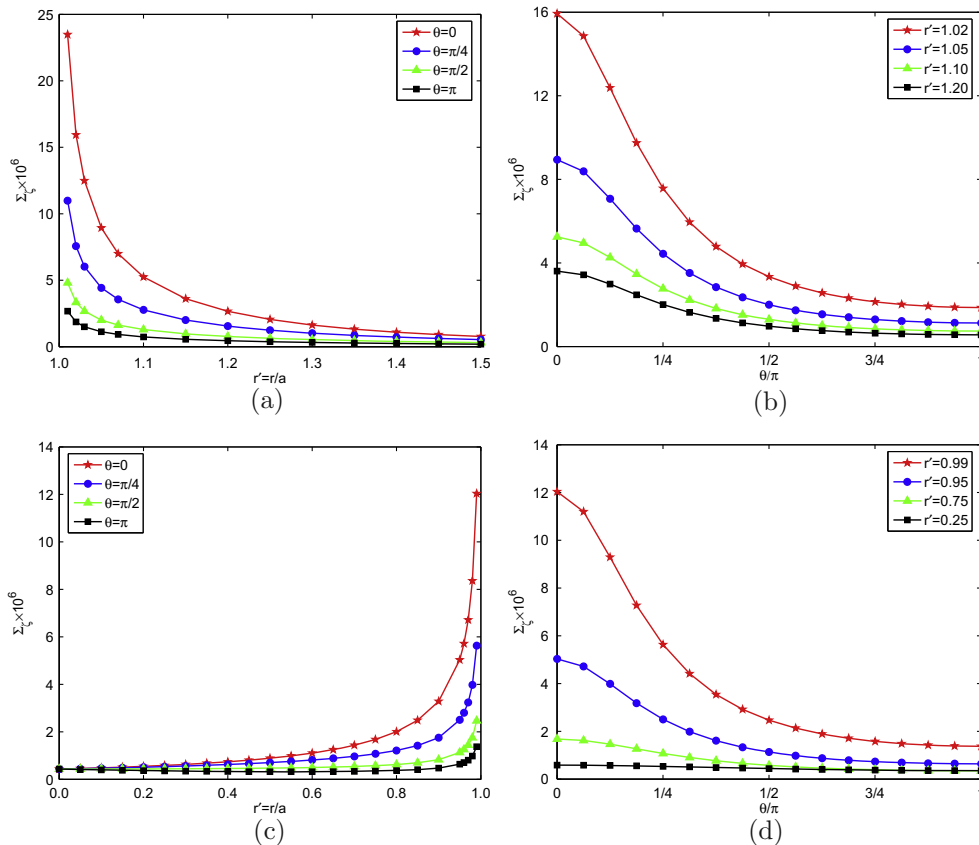characterizes the effect of the phonon–phason effect.

Fig. 3. The dimensionless normal stress component Σ_ζ as functions of r' (a, c) and θ/π (b, d) for penny-shaped crack (a, b) and external circular crack (b, d). Data are for $\lambda = 0.50$ for the penny-shaped crack and $\lambda = 2.0$ for the latter.
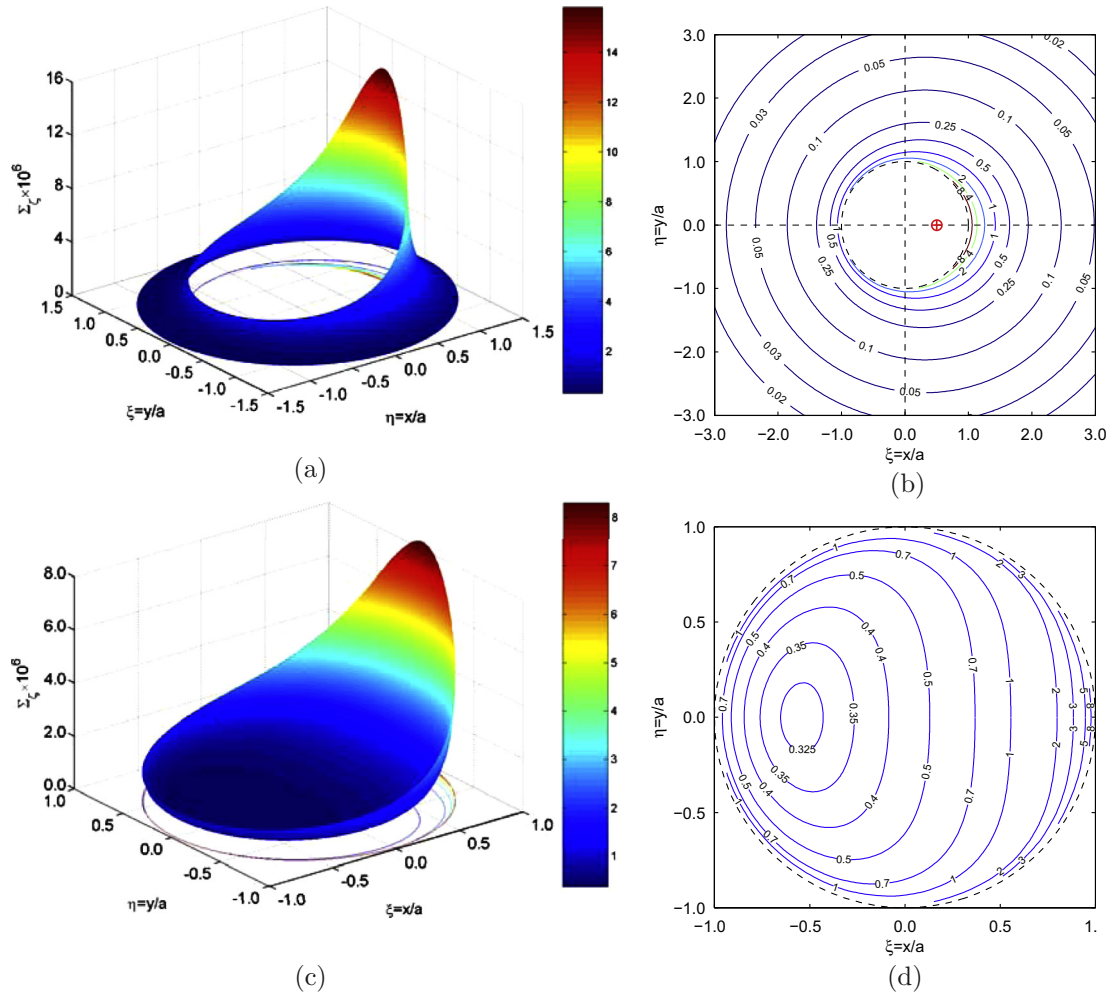
Fig. 4. The 3D figure (a, c) and the contour (b, d) of the dimensionless normal stress components Σ_ζ on the intact region $\overline{S}$ for the penny-shaped crack (a, b) and circular external crack (c, d). Data are for $\lambda = 0.50$ for former and $\lambda = 2.0$ for the latter. The symbol $\oplus$ denotes the position of the external load in (b), and the dashed lines in (b) and (d) stand for the edges of the circular cracks.
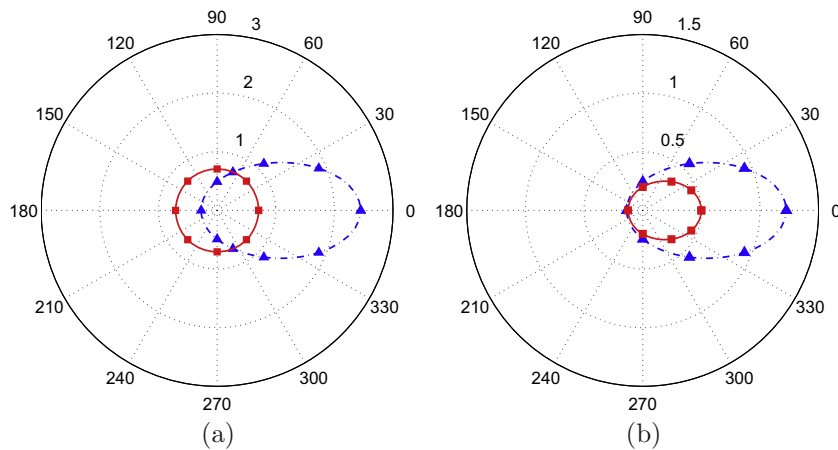

Fig. 5. The distributions of the dimensionless SIF $K'_{1I} \times 10^6$ in the polar system, for the penny-shaped crack (a) and the external circular crack (b). The solid and dashed lines represents the data for $\lambda = 0.0$ and 0.5 for the former crack, and for $\lambda = 2.0$ and 3.0 for the latter. The symbols ($\triangle$) and ($\square$) stand for the elastic results given by Fabrikant (1989) and Fabrikant et al. (1994).
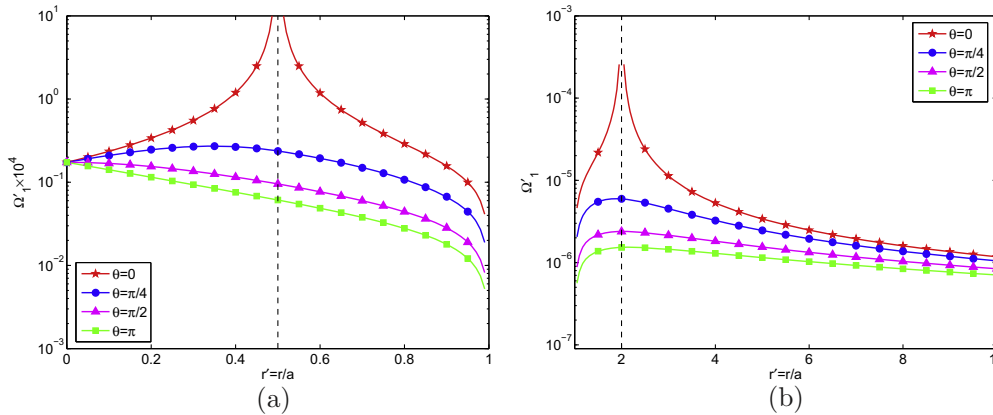
Fig. 6. The variations of the dimensionless CSDs Ω'_1 for the penny-shaped crack (a) and the external circular crack (b) with the dimensionless coordinate r'. Data are for $\lambda = 0.5$ (a) and $\lambda = 2.0$ (b).

8. Concluding remarks

The problem of a planar crack contained in an infinite medium of 1D hexagonal QCs has been analytically treated by means of the potential theory method in conjunction with the general solutions of 3D static problems. In particular, a new potential has been introduced to account for the phonon field. Corresponding boundary integral equations, which are of primary significance for boundary element method, are established.

When the lips of crack with special configurations (penny-shaped, external circular and half-infinite plane) are subjected to non-axisymmetric external concentrated forces, the resulting phonon and phason elastic fields are expressed completely and exactly in terms of some elementary functions. The physical quantities such as SIFs and CSDs, which play an important role in crack analysis, have been explicitly derived. In particular, no interactions between the phonon and phason fields are observed in SIFs.

For the crack subjected to arbitrarily distributed loading, corresponding physical quantities can be obtained by integrating the fundamental solution over the crack surface. In the present study, three concrete examples, which are classical in the context of the fracture mechanics, are presented to illustrate applications of the fundamental solutions. Of particular interest is that the energy release rate for the three common cracks bears an identical expressions in terms of stress intensity factors.

It is also interesting that the fundamental solutions for the three cracks are of a uniform form. This means intrinsic relations must exist among the solutions for these three cracks, for example, the solution for half-infinite plane crack can be exacted from those for penny-shaped crack through a limiting procedure. However, the relations between penny-shaped and external circular cracks remain unknown.

It should be noted that the results presented in this work are valid under the condition that the eigenvalues defined in Section 2 are all distinct. However, if any two, or more than two, of them are equal, the corresponding results can be extracted from the present ones through the limiting procedure suggested by Fabrikant (1989) using L'Hôspital rule.

Appendix A

The constants a, b, c and d involved in the characteristic equation (2) are related to the material properties as follows (Chen et al., 2004)

$$a = c_{44}(R_2^2 - c_{33}K_1), \ d = c_{11}(R_3^2 - c_{44}K_2),$$
$$b = c_{33}\left[-c_{44}K_2 + (R_1 + R_3)^2\right] - K_1[c_{11}c_{33} + c_{44}^2 - (c_{13} + c_{44})^2]$$
$$+ R_2[2c_{44}R_3 + c_{11}R_2 - 2(c_{13} + c_{44})(R_1 + R_3)],$$
$$c = c_{44}\left[-c_{11}K_1 + (R_1 + R_3)^2\right] - K_2[c_{11}c_{33} + c_{44}^2 - (c_{13} + c_{44})^2]$$
$$+ R_3[2c_{11}R_2 + c_{44}R_3 - 2(c_{13} + c_{44})(R_1 + R_3)].$$

In order to specify the constants in (3) and (5), we introduce the following constants

$$m_1 = -K_2(c_{13} + c_{44}) + R_3(R_1 + R_3), \ m_2 = -K_1(c_{13} + c_{44}) + R_2(R_1 + R_3),$$
$$m_3 = -c_{11}K_1 - c_{44}K_2 + (R_1 + R_3)^2, \ m_4 = c_{11}R_2 - c_{44}R_1 - c_{13}(R_1 + R_3),$$
$$\beta_{1j} = m_2 s_j^2 - m_1, \ \beta_{2j} = -c_{11}K_2 - m_3 s_j^2 - c_{44}K_1 s_j^4, \ \beta_{3j} = c_{11}R_3 - m_4 s_j^2 + c_{44}R_2 s_j^4.$$

The constants in (3) and (5) are defined as

$$\alpha_{1j} = \frac{\beta_{2j}}{\beta_{1j}s_j}, \quad \alpha_{2j} = \frac{\beta_{3j}}{\beta_{1j}s_j}, \quad \varpi_j = c_{12} + c_{13}\alpha_{1j}s_j + R_1\alpha_{2j}s_j, \quad \vartheta_1 = c_{44},$$
$$\gamma_{1j} = c_{13} + c_{33}\alpha_{1j}s_j + R_2\alpha_{2j}s_j, \quad \vartheta_2 = R_3, \quad \gamma_{2j} = R_1 + R_2\alpha_{1j}s_j + K_1\alpha_{2j}s_j.$$

Appendix B

Here, the derivatives of Green's function $K(M; N_0)$ in (18) are given case by case for the three typical cracks.

B.1. Penny-shaped crack

The derivatives of the Green's function, which are also involved in (20), have been derived by Fabrikant (1989) as

$$\bigwedge K = 2\pi f_1^{(p)}(z) = \frac{2\pi}{\bar{t}}\left[\frac{z}{R_0}\arctan\frac{h}{R_0} - \frac{\sqrt{a^2 - r_0^2}}{\bar{s}}\arctan\frac{\bar{s}}{\sqrt{l_2^2 - a^2}}\right],$$

$$\text{(B-1a)}$$

$$\frac{\partial K}{\partial z} = 2\pi f_2^{(p)}(z) = -\frac{2\pi}{R_0}\arctan\frac{h}{R_0}, \tag{B-1b}$$

$$\frac{\partial^2 K}{\partial z^2} = 2\pi f_3^{(p)}(z) = 2\pi\left[\frac{z}{R_0^3}\arctan\frac{h}{R_0} - \frac{h}{z(R_0^2+h^2)}\left(\frac{r^2-l_1^2}{l_2^2-l_1^2}-\frac{z^2}{R_0^2}\right)\right], \tag{B-1c}$$

$$\bigwedge^2 K = 2\pi f_4^{(p)}(z) = 2\pi\left\{\frac{\sqrt{a^2-r_0^2}}{\bar{t}\bar{s}}\left(\frac{2}{\bar{t}}-\frac{r_0 e^{i\theta_0}}{\bar{s}^2}\right)\arctan\frac{\bar{s}}{\sqrt{l_2^2-a^2}}\right.$$
$$-\frac{z(3R_0^2-z^2)}{\bar{t}^2 R_0^3}\arctan\frac{h}{R_0}+\frac{\sqrt{a^2-r_0^2}\sqrt{l_2^2-a^2}}{\bar{t}\bar{s}^2\left[l_2^2-rr_0 e^{-i(\theta-\theta_0)}\right]}$$
$$\left.-\frac{zh}{(R_0^2+h^2)}\left[\frac{t}{\bar{t}R_0^2}-\frac{r^2 e^{i2\theta}}{(l_2^2-l_1^2)(l_2^2-r^2)}\right]\right\}, \tag{B-1d}$$

$$\bigwedge\frac{\partial K}{\partial z} = 2\pi f_5^{(p)}(z)$$
$$= 2\pi\left[\frac{t}{R_0^3}\arctan\frac{h}{R_0}+\frac{zh}{R_0^2+h^2}\left(\frac{re^{i\theta}}{l_2^2-l_1^2}+\frac{t}{R_0^2}\right)\right], \tag{B-1e}$$

where the over bar stands for the conjugate of a complex variable, and

$$t = re^{i\theta}-r_0 e^{i\theta_0},\quad h = \frac{\sqrt{a^2-r_0^2}\sqrt{a^2-l_1^2}}{a},$$
$$\bar{s} = \sqrt{a^2-rr_0 e^{-i(\theta-\theta_0)}},$$
$$R_0 = \sqrt{r^2+r_0^2-2rr_0\cos(\theta-\theta_0)+z^2},$$
$$l_1 = \frac{1}{2}\left[\sqrt{(r+a)^2+z^2}-\sqrt{(r-a)^2+z^2}\right],$$
$$l_2 = \frac{1}{2}\left[\sqrt{(r+a)^2+z^2}+\sqrt{(r-a)^2+z^2}\right]. \tag{B-2}$$

In addition, the characteristic lengths h, l_1 and l_2 have the following properties

$$l_1 \to \min(a,r),\quad l_2 \to \max(a,r),$$
$$h \to \frac{\sqrt{a^2-r_0^2}\sqrt{a^2-\min^2(a,r)}}{a},\quad \frac{h}{z}\to\sqrt{\frac{a^2-r_0^2}{\max^2(a,r)-a^2}}, \tag{B-3}$$

when z approaches to 0.

It is noted that, the variables r_0 and θ_0 should be replaced by r_m and θ_m, respectively, when the function $f_j^{(p)}(z)$ in (B-1) are replaced by $f_{jm}^{(p)}(z)$ in (20).

B.2. External circular crack

We can define the derivatives of the Green's function for external circular crack by referring to the article (Fabrikant et al., 1994) as

$$\bigwedge K = 2\pi f_1^{(e)}(z) = \frac{2\pi}{\bar{t}}\left\{\frac{z}{R_0}\arctan\frac{J}{R_0}-\arctan\frac{\sqrt{r_0^2-a^2}}{a}-\frac{\sqrt{r_0^2-a^2}}{\bar{s}'}\right.$$
$$\left.\left[\arctan\frac{\bar{s}'}{\sqrt{a^2-l_1^2}}-\arctan\frac{\bar{s}'}{a}\right]\right\}, \tag{B-4a}$$

$$\frac{\partial K}{\partial z} = 2\pi f_2^{(e)}(z) = -\frac{2\pi}{R_0}\arctan\frac{J}{R_0}, \tag{B-4b}$$

$$\frac{\partial^2 K}{\partial z^2} = 2\pi f_3^{(e)}(z) = 2\pi\left[\frac{z}{R_0^3}\arctan\frac{J}{R_0}+\frac{J}{z(R_0^2+J^2)}\left(\frac{z^2}{R_0^2}-\frac{l_2^2-r^2}{l_2^2-l_1^2}\right)\right], \tag{B-4c}$$

$$\bigwedge^2 K = 2\pi f_4^{(e)}(z) = 2\pi\left\{\frac{\sqrt{r_0^2-a^2}}{\bar{t}\bar{s}'}\left(\frac{2}{\bar{t}}+\frac{r_0 e^{i\theta_0}}{\bar{s}'^2}\right)\left[\arctan\frac{\bar{s}'}{\sqrt{a^2-l_1^2}}\right.\right.$$
$$\left.-\arctan\frac{\bar{s}'}{a}\right]+\frac{a\sqrt{r_0^2-a^2}}{\bar{t}\bar{s}'re^{-i\theta}}-\frac{z(3R_0^2-z^2)}{\bar{t}^2 R_0^3}\arctan\frac{J}{R_0}$$
$$+\frac{\sqrt{r_0^2-a^2}\sqrt{a^2-l_1^2}r_0 e^{i\theta_0}}{\bar{t}\bar{s}'^2\left[l_1^2-rr_0 e^{-i(\theta-\theta_0)}\right]}+\frac{2}{\bar{t}^2}\arctan\frac{\sqrt{r_0^2-a^2}}{a}$$
$$\left.+\frac{zJ}{R_0^2+J^2}\left[\frac{r^2 e^{i2\theta_0}}{(l_2^2-l_1^2)\sqrt{r^2-l_1^2}}-\frac{t}{\bar{t}R_0^2}\right]\right\}, \tag{B-4d}$$

$$\bigwedge\frac{\partial K}{\partial z} = 2\pi f_5^{(e)}(z) = 2\pi\left[\frac{t}{R_0^3}\arctan\frac{J}{R_0}-\frac{J}{R_0^2+J^2}\left(\frac{t}{R_0^2}-\frac{re^{i\theta_0}}{l_2^2-l_1^2}\right)\right], \tag{B-4e}$$

where R_0, t and $l_{1,2}$ are defined in (B-2), and

$$s' = \sqrt{rr_0 e^{-i(\theta-\theta_0)}-a^2},\quad J = \sqrt{(l_2^2-a^2)(r_0^2-a^2)}/a. \tag{B-5}$$

With the property of the characteristic lengths l_1 and l_2, we can obtain that

$$\lim_{z\to 0}\frac{J}{z} = \sqrt{\frac{r_0^2-a^2}{a^2-\min^2(a,r)}}. \tag{B-6}$$

B.3. Half-infinite plane crack

The derivatives of the Green's functions in (18) and the functions involved in (20) for the half-infinite plane crack are of the following form (Fabrikant and Karapetian, 1994)

$$\bigwedge K = 2\pi f_1^{(h)}(z) = \frac{2\pi}{\bar{t}}\left[\frac{z}{R_0}\arctan\frac{h^*}{R_0}-c\arctan\sqrt{\frac{\bar{s}^*}{-2l_1^*}}\right], \tag{B-7a}$$

$$\frac{\partial K}{\partial z} = 2\pi f_2^{(h)}(z) = -\frac{2\pi}{R_0}\arctan\frac{h^*}{R_0}, \tag{B-7b}$$

$$\frac{\partial^2 K}{\partial z^2} = 2\pi f_3^{(h)}(z) = 2\pi\left[\frac{z}{R_0^3}\arctan\frac{h^*}{R_0}-\frac{h^*}{z(R_0^2+h^{*2})}\left(\frac{l_1^*}{l_1^*-l_2^*}-\frac{z^2}{R_0^2}\right)\right], \tag{B-7c}$$

$$\bigwedge^2 K = 2\pi f_4^{(h)}(z) = 2\pi\left\{-\frac{2\sqrt{y_0 l_1^*}}{\bar{t}\bar{s}(\bar{s}^*-2l_1^*)}+\frac{c}{\bar{t}}\left(\frac{i}{\bar{s}^*}+\frac{2}{\bar{t}}\right)\arctan\sqrt{\frac{\bar{s}^*}{-2l_1^*}}\right.$$
$$\left.-\frac{z(3R_0^2-z^2)}{\bar{t}^2 R_0^3}\arctan\frac{h^*}{R_0}-\frac{zh^*}{R_0^2+h^{*2}}\left[\frac{t}{\bar{t}R_0^2}+\frac{1}{4l_2^*(l_2^*-l_1^*)}\right]\right\}, \tag{B-7d}$$

$$\bigwedge\frac{\partial K}{\partial z} = 2\pi f_5^{(h)}(z) = 2\pi\left\{\frac{t}{R_0^3}\arctan\frac{h^*}{R_0}+\frac{h^*}{R_0^2+h^{*2}}\left[\frac{i}{2(l_1^*-l_2^*)}+\frac{t}{R_0^2}\right]\right\}, \tag{B-7e}$$

where

$$t = (x - x_0) + \mathrm{i}(y - y_0), \quad s^* = (y + y_0) - \mathrm{i}(x - x_0), \quad c = \sqrt{\frac{2y_0}{\bar{s}^*}}, \qquad \text{(B-8)}$$

$$R_0 = \sqrt{(x - x_0)^2 + (y - y_0)^2 + z^2}, \quad 2l_{1,2}^* = y \mp \sqrt{y^2 + z^2}, \quad h^* = 2\sqrt{y_0 l_2^*}.$$

Appendix C

The elastic field in the infinite QC space weakened by a uniformly load penny-shaped crack can be obtained via the general solutions for crack problem, which were developed by Peng and Fan (2001). Such an approach consists of Fourier series, Hankel transform and duel integral equations, and all the physical quantities are in the form of integral with Bessel functions involved. As a result, the physical quantities seem not to be readily obtained in this way. Owing to its significance of the problem, here, we provide a simple and straightforward method to fulfill our purpose.

Substituting (49) into (10), we can obtain the potentials as (Fabrikant, 1989)

$$\Psi_m(r, z) = -\frac{F_m^0}{2\pi}\left[(2a^2 + 2z^2 - r^2)\arcsin\frac{a}{l_2} - \frac{2a^2 - 3l_1^2}{a}\sqrt{l_2^2 - a^2}\right]. \tag{C-1}$$

According to (3), (5), (9) and (C-1), the corresponding elastic field is obtained through a procedure of differentiation

$$U = \frac{re^{\mathrm{i}\theta}}{\pi}\sum_{j=1}^{3} D_j\left[\frac{a\sqrt{l_{2j}^2 - a^2}}{l_{2j}^2} - \arcsin\frac{a}{l_{2j}}\right], \tag{C-2a}$$

$$u_{zm} = -\frac{2}{\pi}\sum_{j=1}^{3} D_j\alpha_{mj}\left[z_j\arcsin\frac{a}{l_{2j}} - \sqrt{a^2 - l_{1j}^2}\right], \tag{C-2b}$$

$$\sigma_1 = -\frac{4}{\pi}\sum_{j=1}^{3} D_j\varpi_j\left[\arcsin\frac{a}{l_{2j}} - \frac{a\sqrt{l_{2j}^2 - a^2}}{l_{2j}^2 - l_{1j}^2}\right], \tag{C-2c}$$

$$\sigma_2 = -\frac{4c_{66}r^2e^{\mathrm{i}2\theta}}{\pi}\sum_{j=1}^{3} D_j\frac{a\sqrt{l_{2j}^2 - a^2}}{l_{2j}^4(l_{2j}^2 - l_{1j}^2)}, \tag{C-2d}$$

$$\sigma_{zm} = -\frac{2}{\pi}\sum_{j=1}^{3} D_j\gamma_{mj}\left[\arcsin\frac{a}{l_{2j}} - \frac{a\sqrt{l_{2j}^2 - a^2}}{l_{2j}^2 - l_{1j}^2}\right], \tag{C-2e}$$

$$\tau_{zm} = -\frac{2a^2 re^{\mathrm{i}\theta}}{\pi}\sum_{j=1}^{3} D_j s_j\gamma_{mj}\frac{\sqrt{a^2 - l_{1j}^2}}{l_{2j}^2\left(l_{2j}^2 - l_{1j}^2\right)}, \tag{C-2f}$$

with $D_j = \sum_{k=1}^{2} d_{jk}F_k^0$ and $l_{mj} = l_m(z_j)$ specified in (B-2). It should be pointed out that the displacements in (C-2b) and the normal stresses in (C-2e) are readily reduced to (49) and (53), respectively, upon letting $z = 0$.

Appendix D

This section is devoted to define the special functions involved in (69) (Gradsbteyn and Ryzbik, 2000)

$$F_1(r; \alpha, \beta) \equiv \int_\beta^r \sqrt{\frac{\alpha^2 - x^2}{r^2 - x^2}}dx = \alpha E(\xi, t) - \beta\sqrt{\frac{r^2 - \beta^2}{\alpha^2 - \beta^2}}(\alpha > r > \beta \geqslant 0),$$

$$F_2(r; \alpha, \beta) \equiv \int_\beta^\alpha \sqrt{\frac{\alpha^2 - x^2}{r^2 - x^2}}dx,$$

$$= rE(\xi, t) - \frac{r^2 - \alpha^2}{r}F(\xi, t) - \beta\sqrt{\frac{\alpha^2 - \beta^2}{r^2 - \beta^2}}(r > \alpha > \beta \geqslant 0),$$

where $F(\xi, t)$ and $E(\xi, t)$ are elliptic functions of the first and second kinds and defined by

$$F(\xi, t) = \int_0^\xi \frac{dx}{\sqrt{1 - t^2\sin^2 x}}, \quad E(\xi, t) = \int_0^\xi \sqrt{1 - t^2\sin^2 x}\,dx, \tag{D-1}$$

with

$$\xi = \begin{cases} \arcsin\frac{\alpha}{r}\sqrt{\frac{r^2 - \beta^2}{\alpha^2 - \beta^2}} & \alpha > r > \beta \\ \arcsin\frac{r}{\alpha}\sqrt{\frac{\alpha^2 - \beta^2}{r^2 - \beta^2}} & r > \alpha > \beta \end{cases}, \quad t = \frac{\min(r, \alpha)}{\max(r, \alpha)}. \tag{D-2}$$

In the limiting case $r \to \beta^+$ with $\alpha > r$, we have the properties

$$\xi \to \frac{\alpha}{r}\sqrt{\frac{r^2 - \beta^2}{\alpha^2 - \beta^2}}, \quad F(\xi, t) \to \xi, \; E(\xi, t) \to \xi.$$

These limits are of significance in predicting the asymptotic behaviors of CSDs.

References

Bochner, S., Chandrasekharan, K., 1949. Fourier Transforms. Princeton University Press, New York.
Chen, W.Q., Ma, Y.L., Ding, H.J., 2004. On three-dimensional elastic problems of one-dimensional hexagonal quasicrystal bodies. Mech. Res. Commun. 31, 633–641.
Colli, S., Mariano, P.M., 2011. The standard description of quasicrystal linear elasticity mayproduce non-physical results. Phys. Lett. A 375, 3335–3339.
Fabrikant, V.I., 1989. Application of Potential Theory in Mechanics: A Section of New Results. Kluwer Academic Publishers, Dordrecht.
Fabrikant, V.I., 1991. Mixed Boundary Value Problem of Potential Theory and Their Applications in Engineering. Kluwer Academic Publishers, Dordrecht.
Fabrikant, V.I., Karapetian, E.N., 1994. Elementary exact method for solving boundary-value problems of potential theory with application to half-plane contact and crack problems. Q. J. Mech. Appl. Math. 47, 159–174.
Fabrikant, V.I., Rubin, B.S., Karapetian, E.N., 1993. Half-plane crack under normal crack: complete solution. J. Eng. Mech. 119, 2238–2251.
Fabrikant, V.I., Rubin, B.S., Karapetian, E.N., 1994. External circular crack under normal load: a complete solution ASME. J. Appl. Mech. 61, 809–814.
Fabrikant, V.I., Rubin, B.S., Karapetian, E.N., 1995. A half-plane crack under tangential load: a complete solution Z. Angew. Math. Mech. 75, 523–534.
Fan, T.Y., 2011. Mathematical Theory of Elasticity of Quasicrystals and Application. Springer-Verlag, Heidelberg.
Fan, T.Y., Mai, Y.W., 2004. Elasticity theory, fracture mechanics, and some relevant thermal properties of quasi-crystalline materials. Appl. Mech. Rev. 57, 325–343.
Fan, T.Y., Tang, Z.Y., Chen, W.Q., 2012. Theory of linear, nonlinear and dynamic fracture for quasicrystal. Eng. Fract. Mech. 82, 185–194.
Gao, Y., Ricoeur, A., 2010. Green's functions for infinite bi-material planes of cubic quasicrystals with imperfect interface. Phys. Lett. A 374, 4354–4358.
Gao, Y., Ricoeur, A., 2011. Three-dimensional Green's functions for two-dimensional quasi-crystal bimaterials. Proc. R. Soc. A 467, 2622–2642.
Gao, Y., Xu, S.P., Zhao, B.S., 2009. General solutions of equilibrium equations for 1D hexagonal quasicrystals. Mech. Res. Commun. 36, 302–308.
Gradsbteyn, I.S., Ryzbik, L.M., 2000. Table of Integrals, Series and Products, sixth edition. Elsevier Pte Ltd, Singapore.
Hinch, E.J., 1991. Perturbation Methods. Combridge Press, Combridge.
Kellogg, O.D., 1929. Foundations of Potential Theory. F. Ungar Publishing, New York.
Kenzari, S., Bonina, D., Dubois, J.M., Fournee, V., 2012. Quasicrystal–polymer composites for selective laser sintering technology. Mater. Des. 35, 691–695.
Landau, L.D., Lifshitz, E.M., 1958. Statistical Physics, second ed. Pergamom Press, New York (English translation).
Li, X.Y., 2012. Fundamental electro-elastic field in an infinite transversely isotropic piezoelectric medium with a permeable external circular crack. Smart Mater. Struct. 21, 12, 065019.
Li, X.Y., 2013. Fundamental solutions of penny-shaped and half-infinite plane cracks embedded in an infinite space of one-dimensional hexagonal quasi-crystal under thermal loading. Proc. R. Soc. A. 469, 20130023.
Li, L.H., Liu, G.T., 2012. Stroh formalism for icosahedral quasicrystal and its application. Phys. Lett. A 376, 987–990.
Mariano, P.M., 2006. Mechanics of quasi-periodic alloys. J. Nonlinear Sci. 6, 45–77.
Mariano, P.M., Planas, J., 2013. Phason self-actions in quasicrystal. Physica D 249, 46–57.
Mariano, P.M., Stazi, F.L., Augusti, G., 2004. Phason effects around a crack in Al–Pb–Mn quasicrystals: stochastic aspects of the phonon–phason coupling. Comput. Struct. 82, 971–983.
Muskhelishvili, N.I., 1963. Some Basic Problems of Mathematical Theory of Elasticity. Noordhoff, Groningen.
Peng, Y.Z., Fan, T.Y., 2001. Crack and indentation problems for one-dimensional hexagonal quasi-crystal. Eur. Phys. J. B 21, 39–44.

Radi, E., Mariano, P.M., 2011. Steady-state propagation of dislocations in quasi-crystals. Proc. R. Soc. A 467, 3490–3508.

Shechtman, D., Blech, I., Gratias, D., Cahn, J.W., 1984. Metallic phase with long-range orientational order and no translational symmetry. Phys. Rev. Lett. 53, 1951–1953.

Stroh, A.N., 1958. Dislocation and cracks in anisotropic elasticity. Philos. Mag. 3, 625–646.

Stroh, A.N., 1962. Steady state problems in anisotropic elasticity. J. Math. Phys. 41, 77–103.

Wang, X., 2004. Eshelby's problem of an inclusion of arbitrary shape in a decagonal quasicrystalline plane or half-plane. Int. J. Eng. Sci. 42, 1911–1930.

Wang, R.H., Yang, W.G., Hu, C.Z., Ding, D.H., 1997. Point and space groups and elastic behaviours of one-dimensional quasi-crystals. J. Phys.: Condens. Matter 9, 2411–2422.

Wu, Y.F., Chen, W.Q., Li, X.Y., 2013. Indentation on one-dimensional hexagonal quasicrystals: general theory and complete exact solutions. Philos. Mag. 93, 858–882.